

## 2D-XAFS imaging of Ce oxidation states in Pt/Ce<sub>2</sub>Zr<sub>2</sub>O<sub>x</sub> particles during oxygen storage and release processes

An assembly of non-uniform particles in a powder is a typical form of a heterogeneous solid catalyst. There are heterogeneous hierarchical structures (morphology, surface structures, domain boundaries, and so forth) in a solid catalyst. The reactivity of a solid catalyst is determined by such structural heterogeneity, but it is still difficult to visualize and understand the real active parts and heterogeneous reaction modes in a heterogeneous solid catalyst.

Ce<sub>2</sub>Zr<sub>2</sub>O<sub>x</sub> (CZ; x = 7–8) solid solution with an ordered arrangement of Ce and Zr atoms has been reported to exhibit excellent oxygen storage/release properties [1]. Almost 90% of the Ce atoms in CZ bulk can participate in the redox process for oxygen storage/release and the structure of CZ changes between oxidized Ce<sub>2</sub>Zr<sub>2</sub>O<sub>8</sub> (Ce<sup>4+</sup>) and reduced Ce<sub>2</sub>Zr<sub>2</sub>O<sub>7</sub> (Ce<sup>3+</sup>). We performed scanning nano-XAFS measurements at the Ce L<sub>III</sub>-edge to visualize the distribution of Ce oxidation states in individual CZ particles and investigated the role of Pt in the oxygen storage/release processes. The nano-XAFS imaging showed the heterogeneous reaction modes and active parts in individual CZ particles for the first time [2].

Scanning nano-XRF and nano-XAFS measurements were conducted at SPRING-8 BL36XU and BL39XU. Hard X-rays from an undulator were monochromatized by Si(111) crystals and focused by Kirkpatrick-Baez

mirrors to a size of 409(h) × 154(v) nm<sup>2</sup> at 6 keV (Fig. 1). A sample enclosed in an XAFS cell with an inert He flow was mounted on an encoded-feedback translation stage (10 nm resolution) at the focal point of the X-ray beam and inclined at a tilt of 30° with respect to the optical path. Incident and fluorescent X-rays were detected by a He-filled ion chamber and a 21-element Ge detector (Canberra, EGPX 40 × 40 × 7-21PIX), respectively. Scanning nano-XRF mappings were measured every 150 nm at 122 energies at the L<sub>III</sub>-edge (5.68–5.80 keV). The Ce valence was calculated by the linear combination fitting of the Ce L<sub>III</sub>-edge nano-XANES spectra of Ce<sub>2</sub>Zr<sub>2</sub>O<sub>7</sub> (Ce<sup>3+</sup>) and Ce<sub>2</sub>Zr<sub>2</sub>O<sub>8</sub> (Ce<sup>4+</sup>) [3].

The CZ particles (0.2–2.0 μm) and commercial micron-size Pt particles (Alfa Aesar, 0.2–1.6 μm) were dispersed on a SiN membrane. The location and distribution of isolated CZ particles were evaluated by SEM analysis and three representative particles (Particle 1: a CZ particle with Pt attached to the side of the particle; Particle 2: a CZ particle with Pt attached to the edge of the particle; Particle 3: a CZ particle without Pt) were selected for nano-XAFS analysis. Oxygen storage and release were processed with a flow of O<sub>2</sub> or 10% H<sub>2</sub>/N<sub>2</sub> at 1,000 mL·min<sup>-1</sup> for 1 h.

Figure 2 shows the BEI-SEM images and the observed 2D mappings of the Ce valence states of Particles 1–3 after the oxygen storage and release

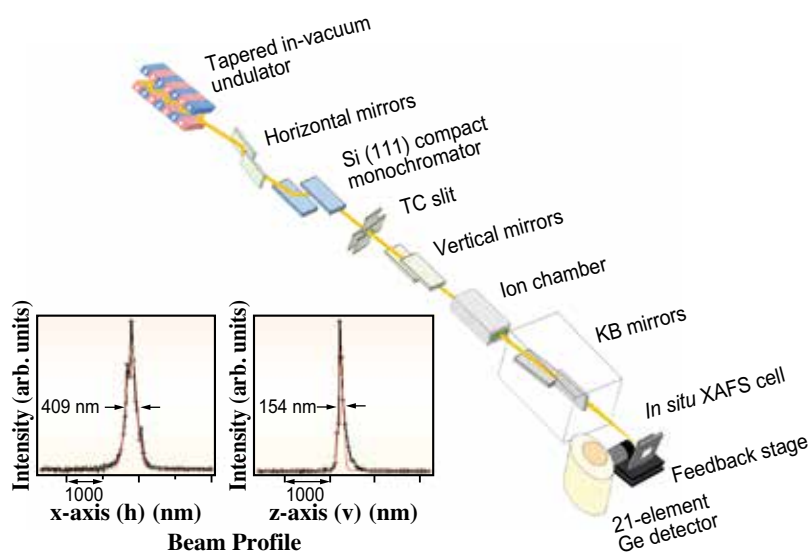


Fig. 1. Experimental setup of nano-XRF and nano-XAFS and the beam profile of the X-ray nanobeam focused by Kirkpatrick-Baez (KB) mirrors at beamline BL36XU.

processes at 423 and 573 K. Black dotted lines show the positions of Pt particles attached to CZ. In the case of Particle 1, in which Pt was located on the side of the CZ particle, the Ce valence state changed smoothly during both oxygen storage and release processes at 573 K (Figs. 2(c-1) and 2(e-1)). Unreacted parts inside the CZ particle were observed for the oxygen storage at 423 K, but were found to be unrelated to the position of Pt (Fig. 2(b-1)).

It should be noted that Particle 2, in which Pt was attached to an edge of the CZ particle, exhibited an isotropic gradient in the Ce oxidation state with respect to the center of the Pt particle for the oxygen release process at 423 K (Fig. 2(d-2)), indicating that the Pt catalyst played a crucial role in the oxygen release by  $H_2$ . These results clearly suggest that the initiation of the oxygen release locally proceeds from the attached Pt catalyst on CZ then oxygen diffusion spreads into the CZ bulk. The scanning nano-XAFS imaging evidenced the significance of the interface between the Pt catalyst and the CZ particle as a preferential oxygen release site. On the other hand, the color change in the CZ particle was found to be unrelated to the position of Pt for the oxygen storage at 423 K (Fig. 2(b-2)), suggesting that the oxygen storage occurred in domains of the CZ particle without the contribution of the Pt catalyst. After oxidation at 573 K, all the Ce species in Particle 2 had fully reacted (Fig. 2(c-2)).

In the case of Particle 3, oxygen storage similarly proceeded even though Pt was not attached on the CZ particle (Fig. 2(b-3)). Differences in the color changes in the CZ particles imply differences in the reactivity of each CZ particle derived from non-uniform domain structures in the CZ particles. In contrast, the oxygen release was too slow at 423 K and was not completed at 573 K (Fig. 2(d/e-3)), suggesting that the absence of Pt strongly affected the reaction rate of the oxygen release.

In conclusion, the nano-XAFS images obtained using hard X-ray nanobeams showed the modes of the changes in the Ce valence state for the oxygen storage/release processes. Practically, novel metal-nanoparticle-attached catalysts on a ceria-based support have been used for three-way conversion systems. Solid support particles intrinsically have structural heterogeneity, and nanoparticle catalysts attaching and spreading on the support surface should make up for the heterogeneous reactivity of each domain structure in the support. Nano-XAFS imaging is promising for providing new insights and a deeper understanding of heterogeneous catalysis and for developing new practical catalyst systems [2].

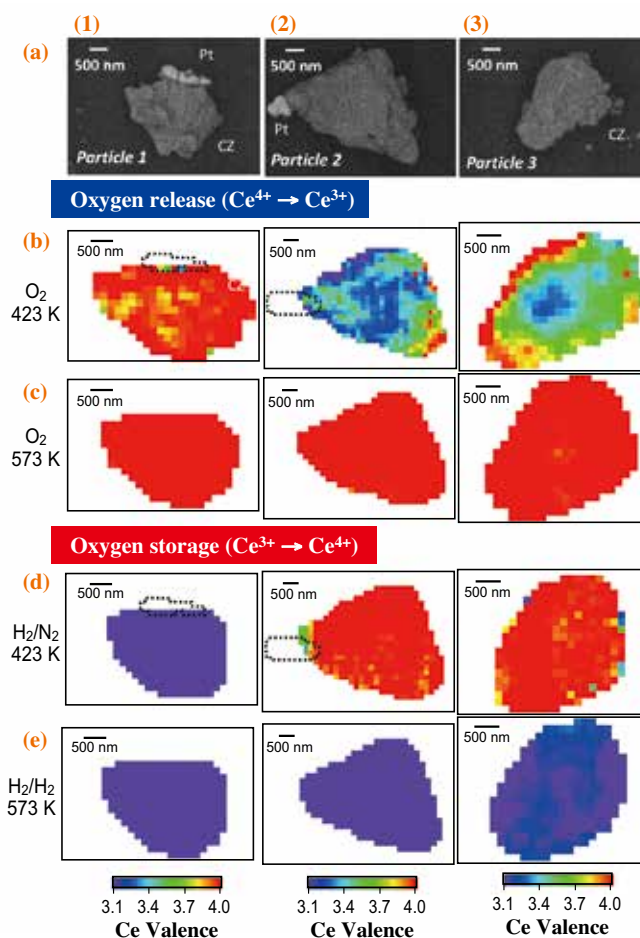


Fig. 2. (a) SEM images (BEI mode) and (b-e) 2D mappings of Ce valence states of Particles 1–3 after the oxygen storage and release processes at 423 and 573 K. Black dotted lines show the positions of Pt particles [2].

Hirosuke Matsui<sup>a</sup>, Nozomu Ishiguro<sup>b</sup> and Mizuki Tada<sup>a,b,\*</sup>

<sup>a</sup>Graduated School of Science & Research Center for Materials Science (RCMS) and Integrated Research Consortium on Chemical Sciences (IRCCS), Nagoya University

<sup>b</sup>RIKEN SPring-8 Center

\*Email: mtada@chem.nagoya-u.ac.jp

## References

- [1] A. Suda *et al.*: J. Ceram. Soc. Jpn. **110** (2002) 126.
- [2] H. Matsui, N. Ishiguro, K. Enomoto, O. Sekizawa, T. Uruga, M. Tada: *Angew. Chem. Int. Ed.* **55** (2016) 12022.
- [3] N. Ishiguro *et al.*: *Chem. Phys. Chem.* **15** (2014) 1563.